Earthq Eng & Eng Vib (2012) 11: 221-232 **DOI**: 10.1007/s11803-012-0112-6

Modified consecutive modal pushover procedure for seismic investigation of one-way asymmetric-plan tall buildings

Faramarz Khoshnoudian† and Mahdi Kiani‡

Department of Civil Engineering, Amirkabir University of Technology, Tehran, Iran

Abstract: The effects of higher modes and torsion have a significant impact on the seismic responses of asymmetric-plan tall buildings. A consecutive modal pushover (CMP) procedure is one of the pushover methods that have been developed to consider these effects. The aim of this paper is to modify the (CMP) analysis procedure to estimate the seismic demands of one-way asymmetric-plan tall buildings with dual systems. An analysis of 10-, 15- and 20-story asymmetric-plan buildings is carried out, and the results from the modified consecutive modal pushover (MCMP) procedure are compared with those obtained from the modal pushover analysis (MPA) procedure and the nonlinear time history analysis (NLTHA). The MCMP estimates of the seismic demands of one–way asymmetric-plan buildings demonstrate a reasonable accuracy, compared to the results obtained from the NLTHA. Furthermore, the accuracy of the MCMP procedure in the prediction of plastic hinge rotations is better than the MPA procedure. The new pushover procedure is also more accurate than the FEMA load distribution and the MPA procedure.

Keywords: modified consecutive modal pushover; seismic demands; nonlinear time history analysis; asymmetric-plan tall buildings; torsion

1 Introduction

Nonlinear static procedures (NSP), as described in various building codes, are the most common tools available for estimating the seismic demands of buildings. However, these procedures are often restricted to a fundamental mode response of a structure. Therefore, they are inappropriate for high-rise buildings with an asymmetric-plan where torsion and higher modes have a significant impact. In the past few decades, several researchers have attempted to develop new pushover procedures to eliminate these limitations. The multi-mode pushover (MMP) method (Sasaki *et al*., 1998), modal pushover analysis (MPA) (Chopra and Goel, 2002), pushover results combinations (PRC) (Moghadam, 2002), incremental response spectrum analysis (IRSA) (Aydinoglu, 2003), upper-bound pushover analysis (Jan *et al*., 2004), modified modal pushover analysis (MMPA) (Chopra *et al*., 2004), an adaptive modal combination (AMC) procedure (Kalkan and Kunnath, 2006), improved modal pushover analysis (Mao *et al*., 2008) and a consecutive modal pushover (CMP) procedure (Poursha *et al*., 2009) have all been proposed to account for the effects of higher modes.

Correspondence to: Mahdi Kiani, Department of Civil Engineering, Amirkabir University of Technology, Tehran, Iran
Tel: (009821) 64543019; Fax: (009821) 64543047
E-mail: mahdikiani@aut.ac.ir
†Associate Professor; ‡M.Sc. Graduate
Received October 30, 2010; **Accepted** March 25, 2012

These enhanced pushover procedures have thus far been developed for symmetric plan buildings; further attempts have been made to improve the capability of these pushover procedures for application to asymmetric-plan buildings. Kilar and Fajfar (1997; 2001), De Stefano and Rutenberg (1998), Faella and Kilar (1998), Moghadam and Tso (1998; 2000), Fujii *et al*. (2004), Barros and Almeida (2005), Chopra and Goel (2004), Fajfar *et al*. (2005; 2008), Lin and Tsai (2007) investigated the application of pushover analysis to asymmetric-plan buildings. In a recent study by Poursha *et al*. (2011), the CMP procedure was extended to one-way asymmetric-plan tall buildings, considering moment resisting frames as a lateral force resisting system. According to this study, by comparing the results obtained from the CMP, MPA and FEMA procedures with those corresponding to nonlinear time history analyses (NLTHA), it was shown that the accuracy of the CMP procedure is more reliable than other methods for estimating seismic demands.

This paper focuses on an evaluation of the modified consecutive modal pushover (MCMP) procedure for one-way asymmetric-plan tall buildings with dual systems. The modal properties of asymmetric-plan buildings and details of the extended CMP procedure are described first. Subsequently, the structural models, ground motions and underlying assumptions are briefly explained. The CMP procedure is next modified to obtain more accurate results (i.e., the MCMP). Finally, the results of the new MCMP procedure are compared with those obtained from FEMA load distributions, the MPA procedure and the nonlinear time history analysis (NLTHA). As a result, the accuracy of the MCMP procedure for estimating plastic hinge rotations in one-way asymmetric-plan tall buildings at both flexible and stiff edges is demonstrated.

2 Governing equations of one-way asymmetric-plan tall buildings

The governing equations of N-story buildings under horizontal earthquake excitations can be expressed as (Poursha *et al*., 2011):

$$\begin{bmatrix} \boldsymbol{m} & \boldsymbol{0} & \boldsymbol{0} \\ \boldsymbol{0} & \boldsymbol{m} & \boldsymbol{0} \\ \boldsymbol{0} & \boldsymbol{0} & \boldsymbol{I}_O \end{bmatrix} \begin{Bmatrix} \ddot{\boldsymbol{u}}_x \\ \ddot{\boldsymbol{u}}_y \\ \ddot{\boldsymbol{u}}_\theta \end{Bmatrix} + f_{\mathrm{s}}(\boldsymbol{u}, \operatorname{sign} \dot{\boldsymbol{u}}) = -\begin{bmatrix} \boldsymbol{m} & \boldsymbol{0} & \boldsymbol{0} \\ \boldsymbol{0} & \boldsymbol{m} & \boldsymbol{0} \\ \boldsymbol{0} & \boldsymbol{0} & \boldsymbol{I}_O \end{bmatrix} \boldsymbol{i}_x \ddot{u}_{\mathrm{gx}}(t) - \begin{bmatrix} \boldsymbol{m} & \boldsymbol{0} & \boldsymbol{0} \\ \boldsymbol{0} & \boldsymbol{m} & \boldsymbol{0} \\ \boldsymbol{0} & \boldsymbol{0} & \boldsymbol{I}_O \end{bmatrix} \boldsymbol{i}_y \ddot{u}_{\mathrm{gy}}(t) \tag{1}$$

where $\boldsymbol{u}_x$, $\boldsymbol{u}_y$ are the x- and y-lateral floor displacements vectors and $\boldsymbol{u}_\theta$ is the torsional floor displacement vector. $\boldsymbol{m}$ is a diagonal mass matrix with $m_{jj} = m_j$, the mass lumped at the jth floor diaphragm. $\boldsymbol{I}_o$ is a diagonal matrix with $I_{jj}=I_{oj}$, the polar moment of inertia corresponding to the jth floor diaphragm about a vertical axis through the center of mass (CM). In the previous equation, the influence vectors associated with the components of ground motion in the x- and y-directions ($\ddot{u}_{gx}(t)$ and $\ddot{u}_{gy}(t)$) are as follows:

$$\boldsymbol{i}_x = \begin{Bmatrix} \boldsymbol{1} \\ \boldsymbol{0} \\ \boldsymbol{0} \end{Bmatrix} \qquad \boldsymbol{i}_y = \begin{Bmatrix} \boldsymbol{0} \\ \boldsymbol{1} \\ \boldsymbol{0} \end{Bmatrix} \tag{2}$$

where each element of the $N\times 1$ vector $\boldsymbol{1}$ is equal to unity and the $N\times 1$ vector $\boldsymbol{0}$ is equal to zero. $f_{\mathrm{s}}(\boldsymbol{u}, \operatorname{sign}\dot{\boldsymbol{u}})$ is the force-deformation relation for a building that deforms into an inelastic range.

Equation (1) can be rewritten for a one-way asymmetric-plan building that is symmetric about the x-axis but asymmetric about the y-axis (see Fig. 1(b)) and subjected to earthquake ground motion in the y-direction:

$$\begin{bmatrix} \boldsymbol{m} & \boldsymbol{0} \\ \boldsymbol{0} & \boldsymbol{I}_o \end{bmatrix} \begin{Bmatrix} \ddot{\boldsymbol{u}}_y \\ \ddot{\boldsymbol{u}}_\theta \end{Bmatrix} + \begin{bmatrix} \boldsymbol{k}_{yy} & \boldsymbol{k}_{y\theta} \\ \boldsymbol{k}_{\theta y} & \boldsymbol{k}_{\theta\theta} \end{bmatrix} \begin{Bmatrix} \boldsymbol{u}_y \\ \boldsymbol{u}_\theta \end{Bmatrix} = -\begin{bmatrix} \boldsymbol{m} & \boldsymbol{0} \\ \boldsymbol{0} & \boldsymbol{I}_o \end{bmatrix} \begin{Bmatrix} \boldsymbol{1} \\ \boldsymbol{0} \end{Bmatrix} \ddot{u}_{\mathrm{gy}} \tag{3}$$

in which $\boldsymbol{k}_{yy}$, $\boldsymbol{k}_{y\theta}$, $\boldsymbol{k}_{\theta y}$ and $\boldsymbol{k}_{\theta\theta}$ are stiffness sub-matrixes. When the radius of gyration for all floor diaphragms is identical ($I_{oj} = m_j r^2$), the sub-matrix $\boldsymbol{I}_o$, can be substituted with $\boldsymbol{I}_o = r^2\boldsymbol{m}$ in the above equation.

The right side of Eq. (3) can be defined as the effective earthquake forces:

$$\boldsymbol{P}_{\mathrm{eff}}(t) = -\begin{Bmatrix} \boldsymbol{m}1 \\ \boldsymbol{0} \end{Bmatrix} \ddot{u}_{\mathrm{gy}}(t) = -\boldsymbol{s}\ddot{u}_{\mathrm{gy}}(t) \tag{4}$$

The time independent part of the spatial distribution of the effective forces in Eq. (4) is the summation of modal inertia force distributions, s_n:

$$\boldsymbol{s} = \begin{Bmatrix} \boldsymbol{m}1 \\ \boldsymbol{0} \end{Bmatrix} = \sum_{n=1}^{2N} \boldsymbol{s}_n = \sum_{n=1}^{2N} \Gamma_n \begin{Bmatrix} \boldsymbol{m}\boldsymbol{\Phi}_{yn} \\ r^2\boldsymbol{m}\boldsymbol{\Phi}_{\theta n} \end{Bmatrix} \tag{5}$$

$\boldsymbol{\Phi}_{yn}$ and $\boldsymbol{\Phi}_{\theta n}$ represent the translation in the y direction and rotation of the N floor about a vertical axis for the nth mode. The modal participating factor, Γ_n, is defined as follows:

$$\Gamma_n = \frac{L_n}{M_n} \tag{6}$$

where

$$L_n = \begin{Bmatrix} \boldsymbol{\Phi}_{yn}^{\mathrm{T}} & \boldsymbol{\Phi}_{\theta n}^{\mathrm{T}} \end{Bmatrix} \begin{Bmatrix} \boldsymbol{m}1 \\ \boldsymbol{0} \end{Bmatrix} = \boldsymbol{\Phi}_{yn}^{\mathrm{T}}\boldsymbol{m}1 = \sum_{j=1}^{N} m_j \phi_{jyn} \tag{7}$$

$$M_n = \begin{Bmatrix} \boldsymbol{\Phi}_{yn}^{\mathrm{T}} & \boldsymbol{\Phi}_{\theta n}^{\mathrm{T}} \end{Bmatrix} \begin{bmatrix} \boldsymbol{m} & \boldsymbol{0} \\ \boldsymbol{0} & r^2\boldsymbol{m} \end{bmatrix} \begin{bmatrix} \boldsymbol{\Phi}_{yn} \\ \boldsymbol{\Phi}_{\theta n} \end{bmatrix} \tag{8}$$

where M_n can be expanded as follows:

$$M_n = \boldsymbol{\Phi}_{yn}^{\mathrm{T}}\boldsymbol{m}\boldsymbol{\Phi}_{yn} + r^2\boldsymbol{\Phi}_{\theta n}^{\mathrm{T}}\boldsymbol{m}\boldsymbol{\Phi}_{\theta n} = \sum_{j=1}^{N} m_j\phi_{jyn}^2 + r^2\sum_{j=1}^{N} m_j\phi_{j\theta n}^2 \tag{9}$$

The following results can be obtained by pre-multiplying each sub-matrix in Eq. (5) by $\boldsymbol{1}^{\mathrm{T}}$:

$$\sum_{n=1}^{2N} M_n^* = \sum_{j=1}^{N} m_j \qquad \sum_{n=1}^{2N} I_{on}^* = 0 \tag{10}$$

in which

$$M_n^* = \frac{(L_n)^2}{M_n} \qquad I_{on}^* = r^2\Gamma_n\boldsymbol{1}^{\mathrm{T}}\boldsymbol{m}\boldsymbol{\Phi}_{\theta n} \tag{11}$$

where M_n^* and I_{on}^* are the effective modal mass and modal static response for the base torque.

3 Modified consecutive modal pushover (MCMP) procedure

The CMP procedure includes multi-stage and conventional single-stage pushover analyses where seismic responses are obtained by enveloping the peak response of each pushover analysis. Note that different pushover analyses can also be used to envelope the results (Fajfar, 2000). In the multi-stage pushover analysis, modal pushover analyses are consecutively performed. As one stage of the analysis is completed, the next stage (pushover analysis using the next mode) begins, where the initial structural states (stress and deformation) are the same as they were at the end of the preceding stage. The lateral force distributions in the multi-stage pushover analysis are obtained using elastic mode shapes. Note that the change in the modal properties of a given structure resulting from inelastic deformations is ignored in the CMP procedure for the lateral force distributions.

In the modified consecutive modal pushover procedure (MCMP), the displacement increment at the roof in each stage of the multi-stage pushover analysis differs from the CMP procedure. The CMP procedure uses the ratio of the effective modal mass to the total seismic mass as the basis for determining the displacement increment; while in the MCMP procedure, the direct influence of the modal vibration periods is also included (Kashani, 2011). The displacement increment, u_{ri}, at the roof in the ith stage of the multi-stage pushover analysis, is determined as follows:

$$u_{ri} = \beta_i \delta_t \tag{12}$$

in which

$$\beta_i = \frac{\Gamma_i D_i}{\sum_{n=1}^{N_s} \Gamma_n D_n} \tag{13}$$

where δ_t is the total target displacement at the roof, β_i is a coefficient related to the modal properties, D_i is the maximum spectrum displacement for a single-degree-of-freedom system equal to the ith mode of vibration and N_s is the number of stages in the multi-stage pushover analysis.

The total target displacement can be determined by utilizing common methods such as the capacity spectrum method (ATC-40, 1996), the displacement coefficient approach (FEMA 273, 1997) and the N2 method (CEN, 2004) or by using the nonlinear dynamic analysis of the structure (Tso and Moghadam, 1998; Mwafy and Elnashai, 2001; Moghadam, 2002). In this investigation, the total target displacement is obtained by using the nonlinear dynamic analysis of the structure.

Lateral modal loads are incrementally applied to the structure in the multi-stage pushover analysis. For this purpose, the lateral modal loads at the end of each stage are preserved and the lateral modal loads at the next stage are added to the previous ones. Generally, the lateral loads ($\boldsymbol{s}_n^* = \boldsymbol{M\Phi}_n$) at each stage of the multi-stage pushover analysis include two lateral forces and one torsional torque at each floor of the asymmetric-plan building (Chopra and Goel, 2004). In one-way asymmetric-plan buildings (asymmetric about the y-axis, for example) in which lateral excitations are in the y- direction, the height-wise lateral incremental loads can be expressed as:

$$\boldsymbol{s}_n^* = \boldsymbol{M\Phi}_n = \begin{bmatrix} \boldsymbol{m} & 0 & 0 \\ 0 & \boldsymbol{m} & 0 \\ 0 & 0 & \boldsymbol{I}_o \end{bmatrix} \begin{Bmatrix} 0 \\ \boldsymbol{\Phi}_{yn} \\ \boldsymbol{\Phi}_{\theta n} \end{Bmatrix} = \begin{Bmatrix} 0 \\ \boldsymbol{m\Phi}_{yn} \\ \boldsymbol{I}_o\boldsymbol{\Phi}_{\theta n} \end{Bmatrix} \tag{14}$$

It is obvious that the lateral loads in the x-direction are equal to zero.

The absolute displacement of the roof (U_{ri}) at the end of each stage of the multi-stage pushover analysis is defined as follows:

$$U_{ri} = \gamma_i \delta_t \tag{15}$$

in which

$$\gamma_i = \sum_{j=1}^{i} \beta_j \qquad i \le N_s \tag{16}$$

The number of required modes (N_s) for the multi-stage pushover analysis is the most important parameter that is modified in the MCMP procedure. The number of modes in the MCMP procedure is based on the number of modes where the sum of the effective modal mass is more than 90% of the total seismic mass of the building.

$$\sum_{i=1}^{N_s} M_i^* \ge 0.9 \sum_{j=1}^{N} m_j \tag{17}$$

where m_j is the seismic mass of the jth floor and N is the number of stories.

In the CMP procedure, a classical single-stage pushover analysis is performed as well as a multi-stage pushover analysis. The single-stage pushover analysis is carried out separately. The CMP procedure utilizes three different lateral load patterns for the single-stage pushover analysis: (1) an inverted triangular load pattern, (2) a uniform force distribution and (3) a force distribution derived from the modal properties of the fundamental effective mode (Poursha *et al.*, 2011). In the MCMP procedure, only the uniform load pattern is used. Consequently, the maximum of the multi-stage and single-stage pushover analysis responses are counted as the seismic demands. The seismic demands obtained from the multi-stage pushover analysis dominate at the mid- and upper-stories of a building; whereas those obtained from the single-stage pushover analysis dominate in the lower stories.

Details of the modified consecutive modal pushover analysis (MCMP) for one-way asymmetric-plan buildings can be expressed as follows:

(1) Compute the natural frequencies, ω_n, and the mode-shapes, $\boldsymbol{\Phi}_n$. The mode shapes are normalized relative to the lateral component of $\boldsymbol{\Phi}_n$ at the roof.

(2) Calculate the incremental lateral forces $\boldsymbol{s}_n^* = \boldsymbol{M\Phi}_n$ in which $\boldsymbol{s}_n^*$ are applied at each floor for the different stages of the multi-stage pushover analysis using Eq. (14).

(3) The total target displacement and the target displacement increment are computed by using Eqs.

(12) and (13).

(4) For each pushover analysis, the gravity loads are considered as an initial condition and then the single-stage and multi-stage pushover analysis are applied to the building until the displacement at the mass center of the roof reaches the total target displacement, δ_t:

1) Perform the single-stage pushover analysis using a uniform lateral load distribution, until the displacement at the roof reaches the total target displacement.

2) The next analysis is the multi-stage pushover analysis. The number of stages in this analysis, N_s, is calculated using Eq. (17).

The first distribution $\boldsymbol{s}_1^* = \boldsymbol{M\Phi}_1$ is applied to the building in the first stage to reach the displacement increment $u_{r1} = \beta_1 \delta_t$. Then, the excitation is continued with the incremental forces $\boldsymbol{s}_2^* = \boldsymbol{M\Phi}_2$ until the displacement increment at the roof equals $u_{r2} = \beta_2 \delta_2$ in the second stage. The pushover analysis is performed next until the number of stages equal N_s and the displacement at the roof reaches the total target displacement (δ_t).At each stage of the multi-stage analysis, the initial condition is the same as the state at the end of the previous stage.

(5) Determine the peak values of the seismic responses such as displacements, story drifts, plastic hinge rotations and axial force of the braces for the single-stage and multi-stage pushover analysis.

(6) The envelope, r, of the peak responses are calculated as :

$$r = \max\{r_s, r_M\} \tag{18}$$

in which r_s, r_M are the peak responses obtained from the single-stage and multi-stage pushover analyses, respectively.

4 Description of structural models

To include a wide range of periods, 10, 15 and 20- story buildings are considered. The structures are symmetric about the x-axis but asymmetric about the y-axis (Fig. 1). These asymmetric structures were obtained from symmetric buildings by modifying the building properties in the plan. In order to create the one-way asymmetric-plan buildings, the center of mass (CM) was displaced relative to the center of stiffness (CS) along the x-axis. The plan of the considered buildings was 15 m by 15 m with three bays in each direction (see Fig. 1) and all the bays were assumed to be 5 m. In spite of the asymmetric-plan, the considered buildings were vertically regular and the story heights were equal to 3.2 m.

As mentioned earlier, the lateral force resisting system of the buildings is presumed to be a dual system. This type of lateral force resisting system involves both a special steel moment resisting frame system (SMRF) and a lateral concentric bracing system that resists lateral excitations. The lateral bracings are located in the mid bays of the exterior sides of the plans (Fig. 1).

Dead and live loads are assumed to be 6.5 and 2.0 kN/m^2. The seismic requirements in the Iranian code of practice (Standard No. 2800-05, 2005) were considered for the seismic design of the buildings; thus, the structures satisfied all the code requirements such as deformation and drift limitations as well as strong column-weak beam criterion. The assumed seismic masses consist of the dead load plus 20% of the live load, and distribution of the mass over the height was considered to be uniform. The studied buildings were designed according to the allowable stress design method (AISC-ASD, 1989). The size, strength and deformation of the panel zone were ignored, but P-Δ (second –order) effects due to the gravity loads were considered.

The eccentricity between the center of mass (CM) and the center of stiffness (CS) were assumed to be 15% of the plan dimension. By modifying the ratio of the floor moment of inertia (I_{oj}) to the floor mass (m_j), two types of asymmetric-plan buildings can be created

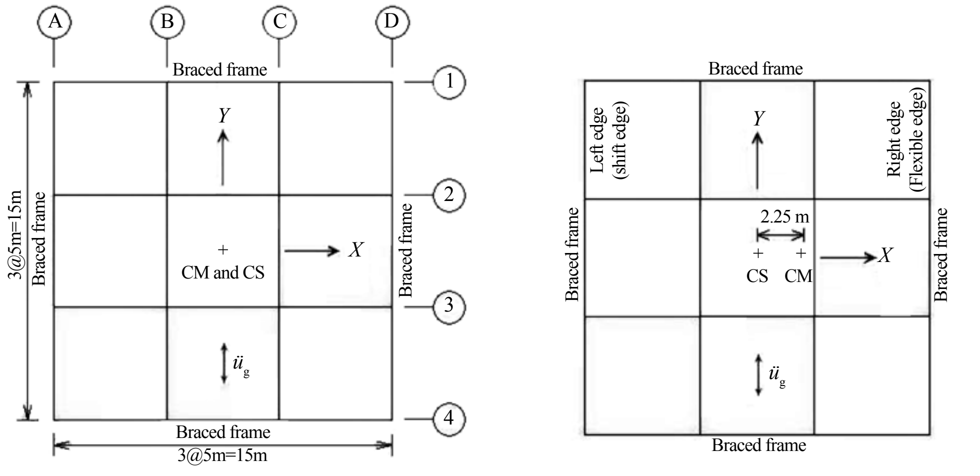

(a) Original symmetric-plan buildings (b) Created one-way asymmetric-plan buildings

Fig. 1 Plan of the analyzed tall buildings

(Chopra and Goel, 2004).

The asymmetric-plan buildings include both torsionally-stiff (TS) and torsionally-flexible (TF) systems, which have different degrees of coupling between translational and torsional motions.

The degrees of coupling between translational and torsional motions in asymmetric-plan buildings can be divided into three groups: torsionally-stiff (TS), torsionally-similarly stiff (TSS) and torsionally-flexible (TF) (Chopra and Goel, 2004). This classification is done on the basis of period ratio (Ω_y), which is defined as the ratio of translational period to torsional period. The period ratio is an important factor in investigating the torsional response of structures (Fajfar *et al*., 2005). In torsionally stiff buildings that have period ratios greater than one, the first and second dominant modes are lateral displacements and torsional rotations, respectively. Torsionally flexible buildings have period ratios less than one and their first and second dominant modes are torsional rotations and lateral displacements,respec tively. In torsionally flexible systems, there is a strong coupling between lateral displacements and torsional rotations so that they have remarkably close modal periods and period ratios near unity.

According to previous investigations on three different groups of asymmetric-plan buildings, for torsionally-similarly stiff (TSS) buildings, various pushover methods are unable to reasonably predict the seismic responses (Chopra and Goel, 2004; Fajfar *et al*., 2005). Therefore, in this paper, torsionally-similarly stiff systems were excluded from the investigations and the considered asymmetric-plan buildings have been restricted to the two first types of buildings. The ratios of the floor moment of inertia between the asymmetric-plan buildings and the corresponding symmetric-plan buildings as well as some specifications of the buildings are listed in Table 1.

5 Analyses and assumptions

In order to evaluate the MCMP procedure, nonlinear time history analyses (NLTHA), modal pushover analyses (MPA) and pushover analyses based on FEMA load patterns have been performed. The peak modal responses obtained from the MPA procedure are combined using the CQC rule. The NLTHA was carried out by using the numerical implicit Wilson-θ time integration method. Seven ground motion records were used in the NLTHA, including Imperial Valley (1979), Victoria (1980), Morgan Hill (1984), Hollister (1986), Trinidad (1980), Northridge (1994) and Duzce (1999). The records were scaled up to 0.9 g and 1.15 g to produce nonlinear responses for the torsionally-stiff and the torsionally-flexible buildings, respectively. The elastic pseudo-acceleration spectrum of the Iranian code of practice for the seismic resistant design of buildings (Standard No. 2800-05, 2005), considering 5% damping ratio, has been used in this investigation. This pseudo-acceleration spectrum has been used as the mean value of the elastic pseudo-acceleration spectra, which can be obtained from ground motion records. The second order (P-Δ) effects were included within all the nonlinear static and dynamic analyses as well as the MPA and the MCMP procedures. In the pushover analyses, the target displacement of the mass center at the roof was computed as the mean value of the peak displacements obtained from the NLTHA at the same point. Otherwise, for each asymmetric plan building, the peak displacement at the mass center of the roof was determined under each ground motion and the mean value of the peak displacements at the roof was calculated as the target displacement of the building. Considering the nonlinear behavior of the structures, the nonlinear hinges corresponding to the acceptance criteria of FEMA-273/356 were defined at the end of the beams. The hysteretic behavior of the hinges was bilinear with 3% post-yield stiffness. The nonlinear analyses were performed by SAP2000 software (Computers and Structures, 2004).

6 Interpretation of results

To estimate the seismic demands of the asymmetric plan buildings and evaluate the accuracy of the MCMP procedure, story displacements, story drifts, plastic hinge rotations and axial forces were computed.

The seismic responses of the asymmetric-plan buildings at the flexible and stiff edges can be used to evaluation the proposed method. Note that displacements and story drifts at the center of mass

Table 1 Details of the analyzed building structures

Number of stories	Total height (m)	Type of buildings	$\frac{(I_{oj})_{\text{unsymmetric}}}{(I_{oj})_{\text{symmetric}}}$	Periods (s)			
				T_1	T_2	T_3	T_4
10	32	TS	1	1.45	1.27	0.87	0.44
		TF	6	2.29	1.37	1.25	0.67
15	48	TS	1	1.85	1.67	1.14	0.54
		TF	6	2.93	1.75	1.67	0.85
20	64	TS	1	2.26	2.24	1.42	0.74
		TF	6	3.7	2.26	2.11	1.25

(CM) are not presented here due to space limitations. Moreover, the accuracy of the MCMP results was examined by comparing them with the exact results obtained from NLTHA. Therefore, the mean value of the maximum responses of the NLTHA at the critical sides of the buildings plan and the mean value plus the standard deviation as well as predictions from other pushover methods (MPA and FEMA load patterns for further examination) are presented.

According to the results obtained from the NLTHA, displacements at the flexible edge of the torsionally stiff buildings, compared with the displacement of the mass center, increase; however, this effect at the stiff edge is the inverse (Fig. 2). Compared with the displacement of the mass center in torsionally flexible buildings, the displacements decreased at the flexible edge and increased at the stiff edge. The latter trends from asymmetric-plan buildings are due to their properties and have been noted in recent investigations (Fajfar *et al*., 2005; Marusic and Fajfar, 2005; Perus and Fajfar 2005; Poursha *et al*., 2011). Figures 2 and 3 illustrate the top normalized displacements in torsionally stiff and torsionally flexible buildings. Normalized displacements are obtained by dividing the displacement on any point of the floor by the CM displacement. As seen in Fig. 2, the displacement response predicted by the MCMP and the MPA procedures at the flexible edge of the torsionally stiff buildings increases and at the stiff edge decreases.

In the same way, according to Fig. 3, the displacement response estimated by the MCMP and MPA procedures at the flexible edge of the torsionally flexible buildings decreases and at the stiff edge increases. These trends are also observed for the the NLTHA. Therefore, the results confirm the ability of the aforementioned procedures to estimate amplification or de-amplification of displacements at critical sides of asymmetric-plan buildings with dual systems due to torsional effects, since they contemplate the influence of the higher modes.

In Figs. 4 and 5, the displacements at the stiff and flexible sides of the asymmetric-plan buildings are illustrated. According to these figures, the pushover method predictions at the flexible edge of the torsionally stiff and flexible systems are consistent with the results of the NLTHA. At the stiff edge of the torsionally stiff systems, the displacements obtained from the MCMP procedure are more accurate than the other pushover procedures that underestimated the displacement demands. Similarly, at the stiff edge of the torsionally flexible buildings, the accuracy of the FEMA load patterns is unacceptable, while the MCMP and MPA procedures provide sufficient accuracy and close to the exact values.

A comparison of the story drifts obtained from the MCMP, MPA and NLTHA methods (as an exact solution) indicates that they have better accuracy than those corresponding to the FEMA load patterns (see Figs. 6 and 7). Including the higher mode effects and using a torsional component in the spatial load distributions contributed to this improvement. The story drift ratios

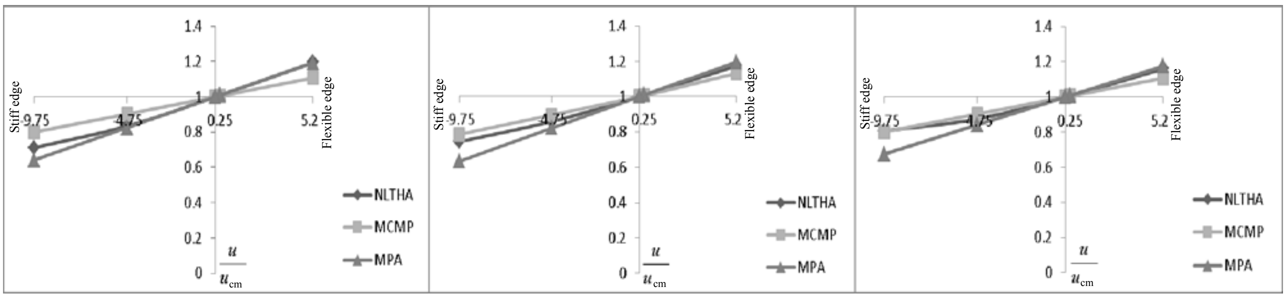

(a) 10 stories (b) 15 stories (c) 20 stories

Fig. 2 Normalized displacements, u/u_{cm}, in the horizontal plane at the top floor level of torsionally-stiff one-way asymmetric-plan buildings

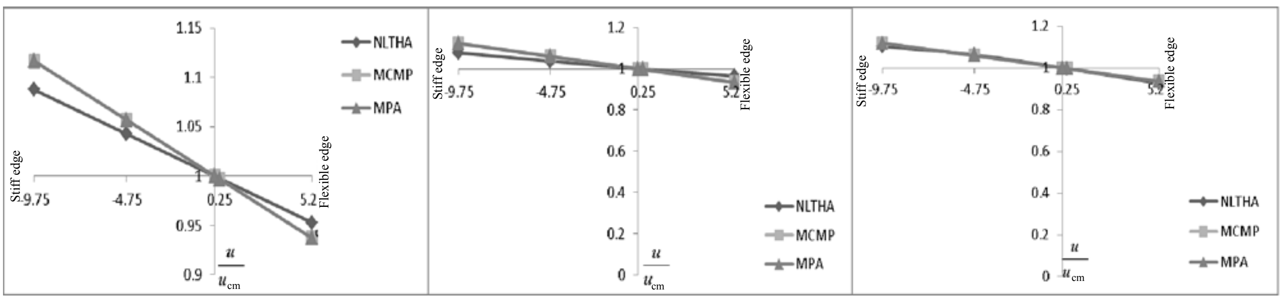

(a) 10 stories (b) 15 stories (c) 20 stories

Fig. 3 Normalized displacements, u/u_{cm}, in the horizontal plane at the top floor level of torsionally-flexible one-way asymmetric-plan buildings

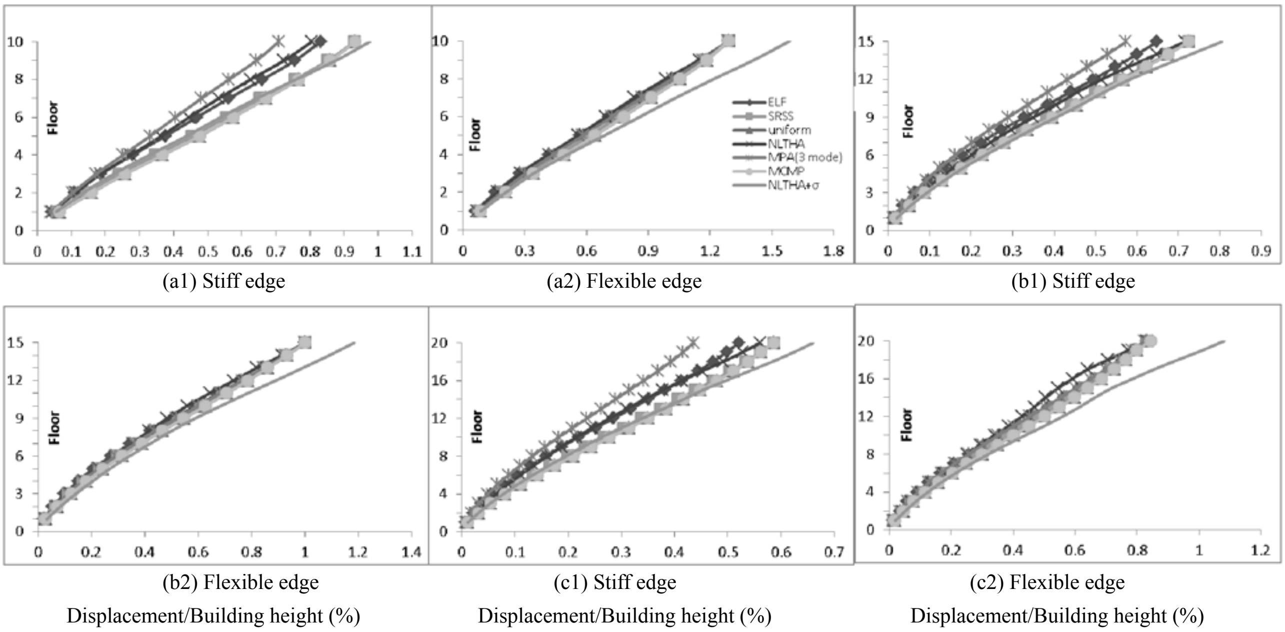

Fig. 4 Height wise variation of the displacements at the left (stiff) and right (flexible) edges of torsionally stiff systems: (a) 10-story building; (b) 15-story building; and (c) 20 story building

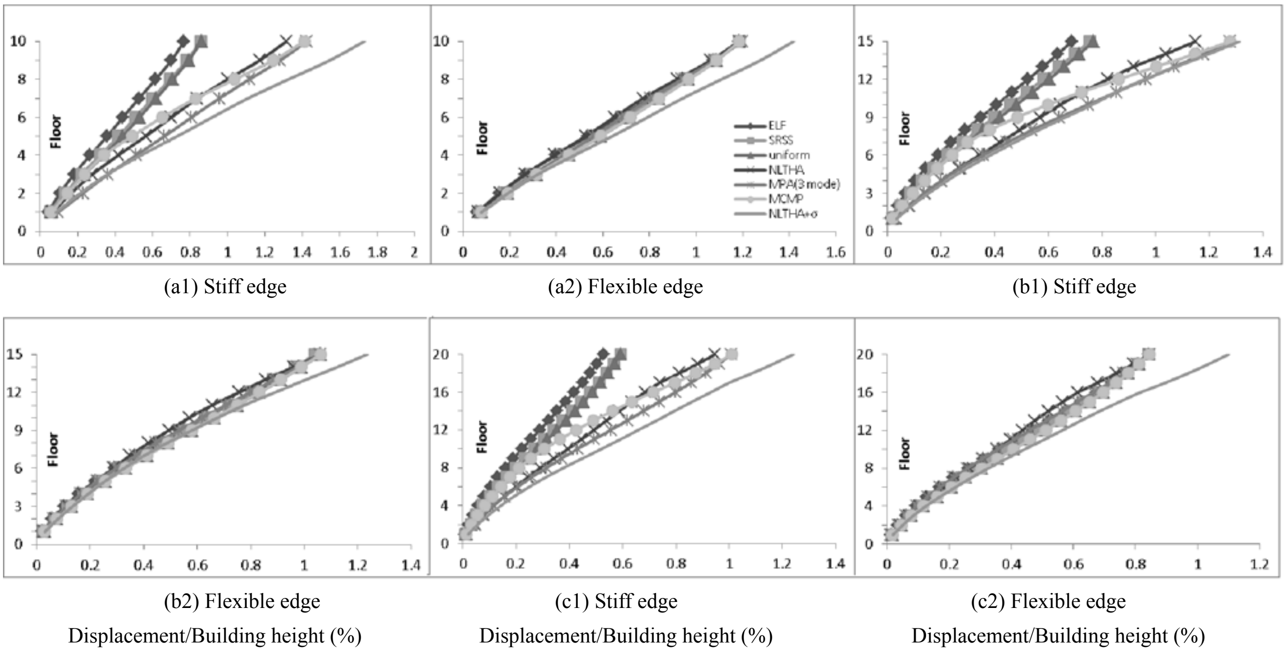

Fig. 5 Height wise variation of the displacements at the left (stiff) and right (flexible) edges of torsionally flexible systems: (a) 10-story building; (b) 15-story building; and (c) 20-story building

obtained from the MCMP procedure are more accurate (sometimes relatively more conservative) than those from the MPA procedure in some cases, especially at the mid and upper stories (Figs. 6 and 7). In some cases, the MPA procedure at the lower stories gives a better prediction when compared with the MCMP procedure. Furthermore, at the stiff edge of the torsionally-stiff buildings, the story drifts from the MPA procedure are less than those obtained from the NLTHA, which is due to determination of the nonlinear response from the resulting the linear responses in this method. Note that three modes are used in the MPA procedure for 10 and 15-story buildings, but four modes are used for the 20-story building. This few number of the used modes in the MPA procedure identifies the negligible effects of the higher modes caused by the rigidity of the considered lateral force resisting system.

Plastic hinge rotations for the exterior beams of the frames at the stiff and flexible edges of the various asymmetric-plan buildings are shown in Figs. 8 and 9. These figures illustrate that the predictions of the MCMP procedure have mostly excellent agreement

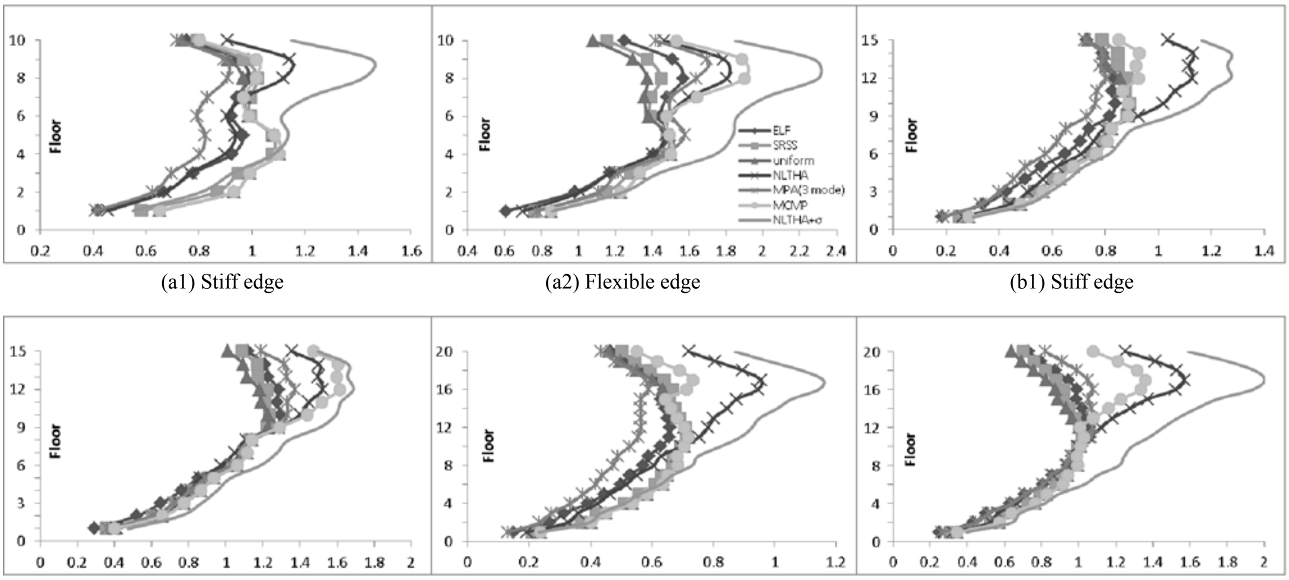

(a1) Stiff edge (a2) Flexible edge (b1) Stiff edge

(b2) Flexible edge (c1) Stiff edge (c2) Flexible edge

Storey drift / Storey height (%) Storey drift / Storey height (%) Storey drift / Storey height (%)

Fig. 6 Height wise variation of the story drifts at the left (stiff) and right (flexible) edges of torsionally stiff systems: (a) 10-story building; (b) 15-story building; and (c) 20-story building

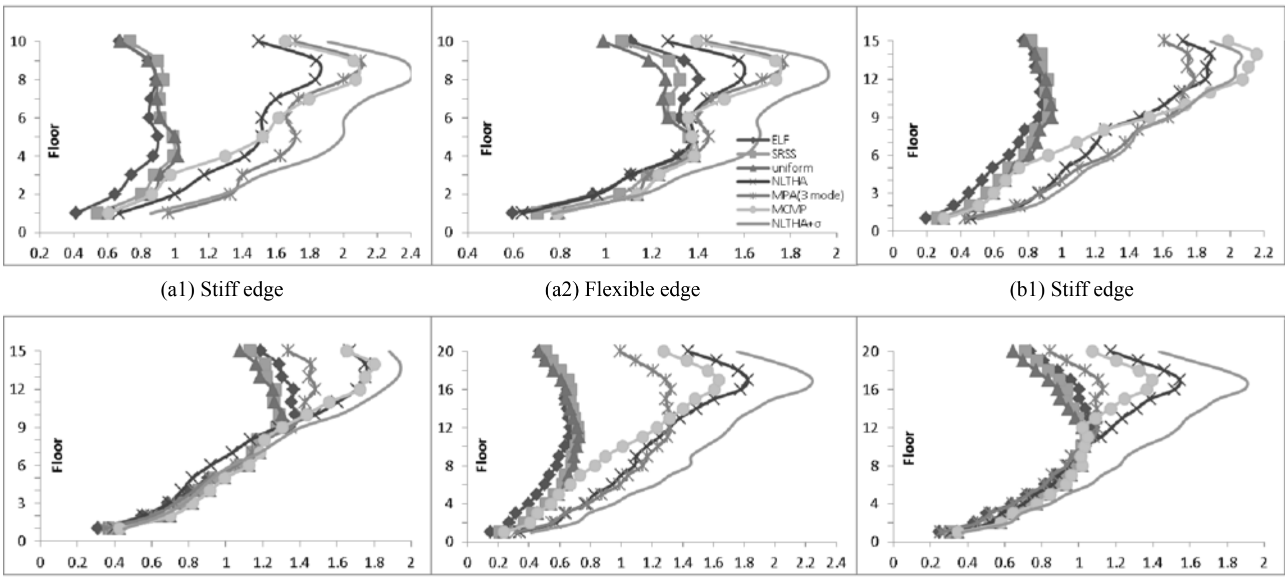

(a1) Stiff edge (a2) Flexible edge (b1) Stiff edge

(b2) Flexible edge (c1) Stiff edge (c2) Flexible edge

Storey drift / Storey height (%) Storey drift / Storey height (%) Storey drift / Storey height (%)

Fig. 7 Height wise variation of the story drifts at the left (stiff) and right (flexible) edges of torsionally flexible systems: (a) 10-story building; (b) 15-story building; and (c) 20-story building

with the results obtained from the NLTHA at the stiff and flexible sides of the buildings. In all of the asymmetric-plan buildings, the MPA procedure and FEMA lateral load patterns are unable to estimate of plastic hinge rotations accurately and their results are considerably underestimated. The MCMP procedure offers a significant improvement in estimating plastic hinge rotations at the stiff and flexible edges of the asymmetric-plan buildings when compared with the MPA procedure. This improvement is obtained by the gradual application of the lateral loads in the MCMP procedure which caused an accumulation of plastic hinge rotations whereas in the MPA procedure the considered buildings remained elastic with the application of the higher modes.

Figures 8(a1), 8(b1), 8(c1) demonstrate that the plastic hinge rotations through the MCMP procedure at the stiff side of the torsionally-stiff buildings are underestimated. In this case, the plastic hinge rotations are very small. In addition, due to the elastic behavior of the structural elements on the stiff sides of the torsionally stiff buildings, the dispersion of the plastic hinge rotations resulting from the NLTHA are greater than those of the flexible edge. On the other hand, the dispersion of the plastic hinge rotations obtained from the NLTHA depends on the intensity of ground motion records. If the intensity of ground motions is small at the stiff edge of the torsionally stiff buildings, the structural elements remain elastic and become inelastic for significantly intense ground motions. For moderate ground motions, the structural elements at the stiff edge under some of the ground motions remains elastic and under others become slightly inelastic. Thus, for torsionally-stiff buildings with moderate ground motions where the

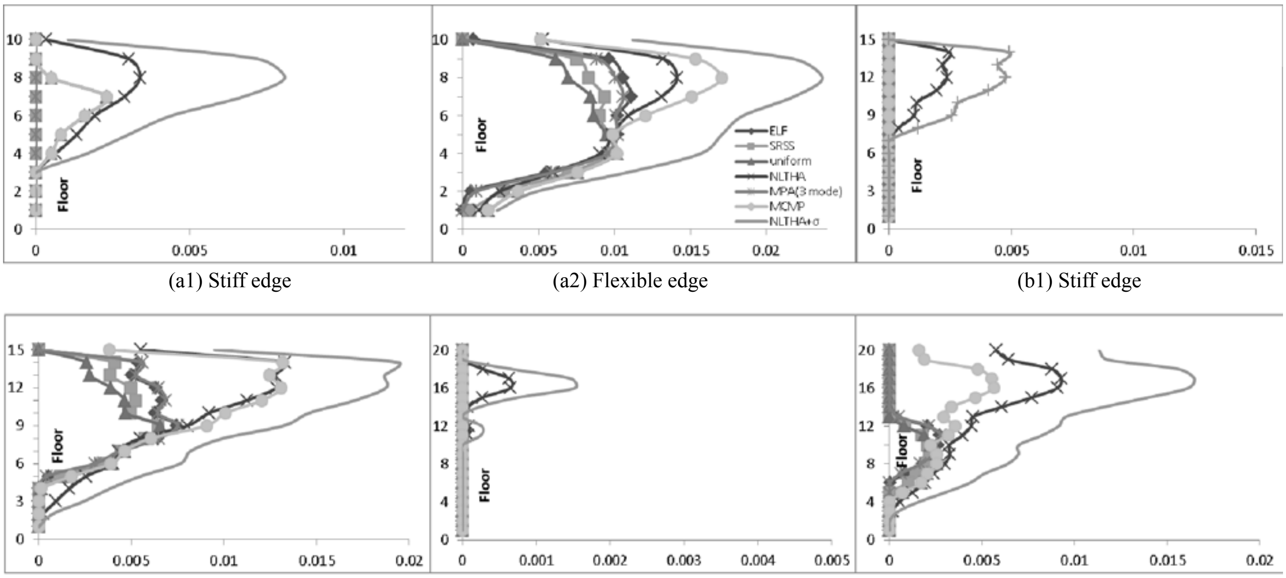

(a1) Stiff edge (a2) Flexible edge (b1) Stiff edge

(b2) Flexible edge (c1) Stiff edge (c2) Flexible edge

Hinge plastic rotation (rad) Hinge plastic rotation (rad) Hinge plastic rotation (rad)

Fig. 8 Height wise variation of the plastic hinges rotation at the left (stiff) and right (flexible) edges of torsionally stiff systems: (a)10-story building; (b) 15-story building; and (c) 20- story building

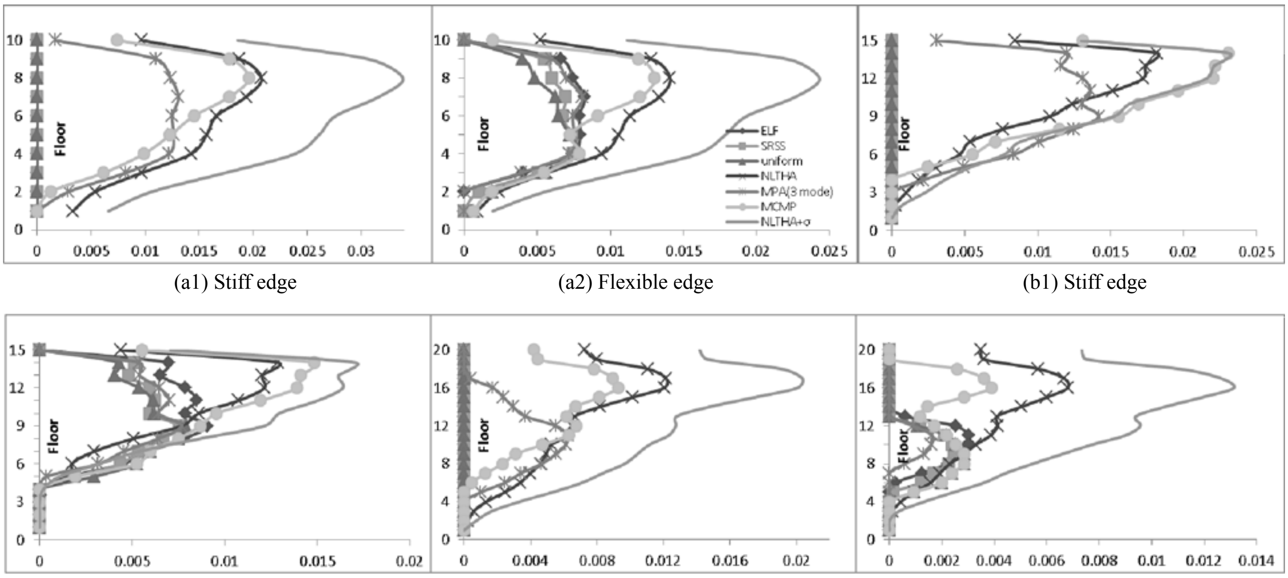

(a1) Stiff edge (a2) Flexible edge (b1) Stiff edge

(b2) Flexible edge (c1) Stiff edge (c2) Flexible edge

Hinge plastic rotation (rad) Hinge plastic rotation (rad) Hinge plastic rotation (rad)

Fig. 9 Height wise variation of the plastic hinges rotation at the left (stiff) and right (flexible) edges of torsionally flexible systems: (a) 10-story building; (b) 15-story building; and (c) 20- story building

ground motions have been scaled up to 0.9 g, the dispersion of plastic hinge rotations is considerable. The plastic hinge rotations are underestimated by the MCMP procedure for the remaining cases, which explains the lateral rigidity of the lateral force resisting system and the different properties of the ground motions.

The plastic hinge rotations obtained from the MCMP procedure may be occasionally overestimated at the upper stories [see Figs. 9(b1), 9(b2) and 8 (a2)]. The occurrence in the range of the mean values of the maximum plastic hinge rotations resulted from the NLTHA and the mean values plus the standard deviation for these cases demonstrated that estimation of the MCMP procedure is acceptable in engineering applications.

Figures 10 and 11 illustrate the axial force of the braces at the stiff and flexible edges of the asymmetric-plan buildings. Generally, the MCMP and the MPA

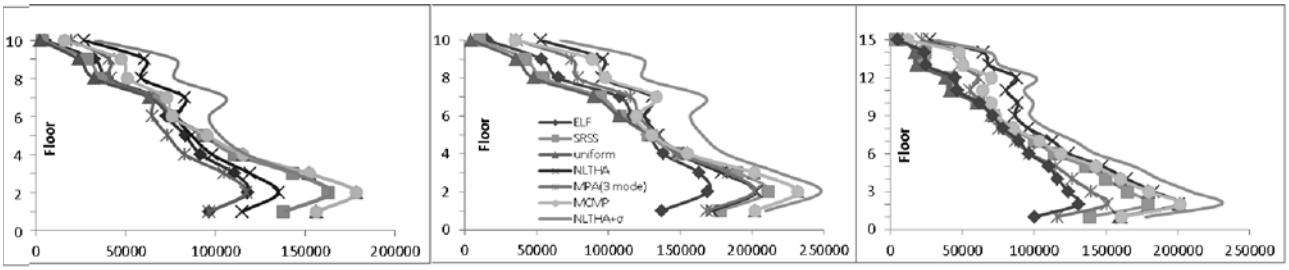

(a1) Stiff edge (a2) Flexible edge (b1) Stiff edge

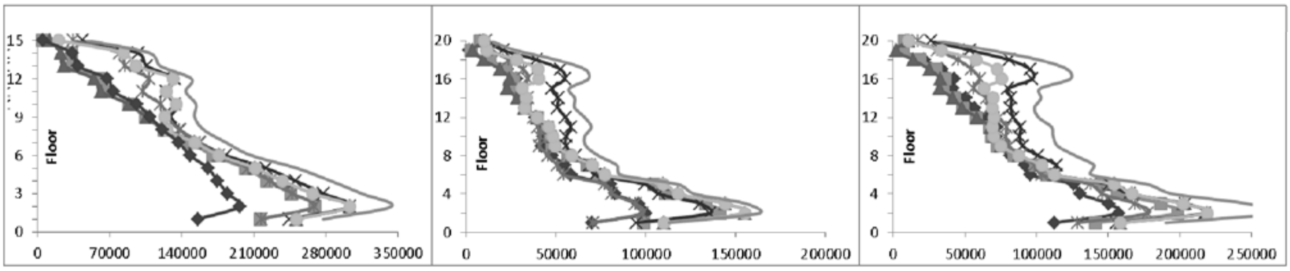

(b2) Flexible edge (c1) Stiff edge (c2) Flexible edge

Axial force (10N) Axial force (10N) Axial force (10N)

Fig.10 Height wise variation of the axial force of braces at the left (stiff) and right (flexible) edges of torsionally-stiff systems: (a) 10-story building; (b) 15-story building; and (c) 20- story building

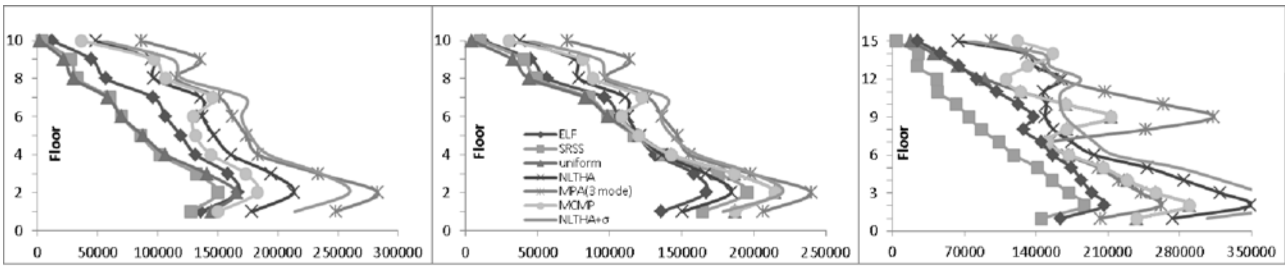

(a1) Stiff edge (a2) Flexible edge (b1) Stiff edge

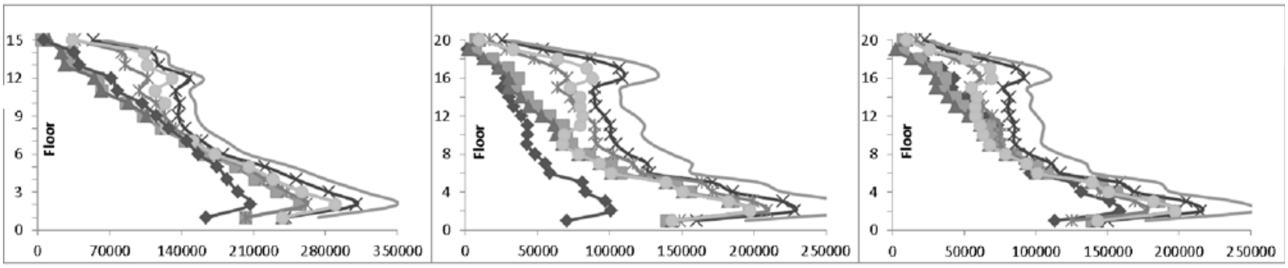

(b2) Flexible edge (c1) Stiff edge (c2) Flexible edge

Axial force (10N) Axial force (10N) Axial force (10N)

Fig. 11 Height wise variation of the braces axial forces at the left (stiff) and right (flexible) edges of torsionally flexible systems: (a) 10-story building; (b) 15-story building; and (c) 20- story building

procedures are able to estimate the axial force of the braces more accurately than the FEMA load patterns. The results obtained from the MCMP in all the stories of the asymmetric-plan buildings are closer to those extracted from the NLTHA, where the MPA prediction of the axial force of the braces is somehow conservative or unconservative.

A mass-eccentric system behavior is similar to the behavior of a stiffness- and strength-eccentric system, where strength relates to stiffness in a linear manner (Perus and Fajfar, 2005). Therefore, the MCMP procedure can be extended to stiffness- and strength-eccentric systems, which was confirmed for the mass-eccentric systems.

7 Conclusions

Based on an extended consecutive modal pushover (CMP) procedure, the modified consecutive modal pushover (MCMP) procedure was proposed for application to one-way asymmetric-plan tall buildings with dual systems as a lateral force resisting system. The seismic demands of the asymmetric-plan tall buildings at the critical edges, i.e., the stiff and flexible edges, was determined and compared with the results of the exact solution from nonlinear time history analysis. The analyses of one-way torsionally stiff and torsionally flexible asymmetric-plan tall buildings with various numbers of stories led to the following conclusions:

(1) The accurate estimation of the amplification or de-amplification of displacements at both edges of the asymmetric-plan tall buildings with the considered lateral force resisting systems show the advantages of the MCMP and MPA procedures.

(2) The accuracy of the MCMP and MPA procedures in predicting floor displacements is the same. However, the results from these two procedures are more reliable than those corresponding to FEMA load patterns such as ELF, SRSS and uniform load patterns. The story drifts obtained from the MCMP procedure, especially at mid- and upper-stories, are more accurate than the MPA procedure and FEMA load patterns for the considered asymmetric-plan buildings. In some cases, the MPA procedure provides a better estimate than the MCMP procedure in the lower stories.

(3) The MCMP procedure achieves remarkable improvement in estimating the plastic hinge rotations of buildings with dual systems. Plastic hinge rotations can indicate deformation of a structure to the inelastic range. Therefore, the MCMP procedure, which is able to accurately predict this parameter, can identify as a method which makes reliable estimates of seismic demands over inelastic range of a building responses.

References

AISC-ASD (1989), "Allowable Stress Design and Plastic Design Specification for Structural Steel Buildings," American Institute of Steel Construction, Chicago, IL.

Applied Technology Council (ATC) (1996), "Seismic Evaluation and Retrofit of Concrete Buildings," *Rep. ATC-40*, ATC, Redwood City, California.

Aydinoglu MN (2003), "An Incremental Response Spectrum Analysis Procedure on Inelastic Spectral Displacements for Multi-mode Seismic Performance Evaluation," *Bulletin of Earthquake Engineering*, **1**: 3–36.

Barros RC and Almeida R (2005), "Pushover Analysis of Asymmetric Three-dimensional Building Frames," *Journal Civil Engineering and Management*, **11**(1): 3–12.

CEN (2004), "Eurocode 8: Design Of Structures for Earthquake Resistance, Part 1: General Rules, Seismic Actions and Rules for Buildings," *Ref. No. EN 1998-1: 2004 (E)*, November 2004, Brussels.

Chopra AK and Goel RK (2002), "A Modal Pushover Analysis Procedure for Estimating Seismic Demands for Buildings," *Earthquake Engineering and Structural Dynamic*, **31**: 561–582.

Chopra AK and Goel RK (2004), "A Modal Pushover Analysis Procedure to Estimate Seismic Demand for Asymmetric–plan Buildings," *Earthquake Engineering and Structural Dynamic*, **33**: 903–927.

Chopra AK, Goel RK and Chintanapakdee C (2004), "Evaluation of a Modified MPA Procedure Assuming Higher Modes as Elastic to Estimate Seismic Demands," *Earthquake Spectra*, **20**(3): 757–778.

Computers & Structures Incorporated (CSI) (2004), *SAP 2000 NL*, Berkeley, CA, U.S.A.

De Stefano M and Rutenberg A (1998), "Predicting the Dynamic Response of Ssymmetric Multi-storey Wall-frame Structures by Pushover Analysis: Two Case Studies," *Proceedings of the 11th European Conference on Earthquake Engineering*, Balkema, Rotterdam.

Faella G and Kilar V (1998), "Asymmetric Multi-storey R/C Frame Structures: Push-over Versus Nonlinear Dynamic Analysis," *Proceedings of the 11th European Conference on Earthquake Engineering*, Balkema, Rotterdam.

Fajfar P (2000), "A Nonlinear Analysis Method for Performance Based Seismic Design," *Earthquake Spectra*, **16**(3): 573–592.

Fajfar P, Marusic D and Perus I (2005), "Torsional Effects in the Pushover-based Seismic Analysis of Buildings," *Journal of Earthquake Engineering*, **9**(6): 831–854.

Fajfar P, Marusic D, Perus and Kereslin M (2008), "The N2 Method for Asymmetric Buildings," *Workshop of Nonlinear Static Methods for Design/ Assessment of 3D Structures*, Lisbon, Portugal.

Federal Emergency Management Agency (FEMA) (1997), "Prestandard and Commentary for Seismic

Rehabilitation of Buildings," *FEMA273*, FEMA, Washington, D.C.

Federal Emergency Management Agency (FEMA) (2000), "Prestandard and Commentary for Seismic Rehabilitation of Buildings," *FEMA356*, FEMA, Washington, D.C.

Fujii K, Nakano Y and Sanada Y (2004), "Simplified Nonlinear Analysis Procedure for Asymmetric Buildings," *Proceeding of the 13th World Conference on Earthquake Engineering*, Vancouver, Canada, Paper No. 149.

Jan TS, Liu MW and Kao YC (2004), "An Upper-bound Pushover Analysis Procedure for Estimating the Seismic Demands of High-rise Buildings," *Engineering Structures*, **26**: 117–128.

Kalkan E and Kunnath SK (2006), "Adaptive Modal Combination Procedure for Nonlinear Static Analysis of Building Structures," *Journal of Structural Engineering*, ASCE, **132**(11): 1721–1731.

Kashani MM (2011),"Evaluation of Consecutive Modal Pushover Procedure for Structural Steel Tall Building with Combination of Moment Resisting Frame System and Concentric Steel Bracing," *M.Sc. Thesis*, Department of Civil Engineering, Amirkabir University of Technology, Tehran, Iran.

Kilar V and Fajfar P (1997), "Simple Push-over Analysis of Asymmetric Buildings," *Earthquake Engineering and Structural Dynamic*, **26**: 233–249.

Kilar V and Fajfar P (2001), " On the Applicability of Pushover Analysis to the Seismic Performance Evaluation of Asymmetric Buildings," *European Earthquake Engineering*, **15**: 20–31.

Lin JL and Tsai KC (2007), "Simplified Seismic Analysis of Asymmetric Building Systems," *Earthquake Engineering and Structural Dynamics*, **36**: 459–479.

Mao Jianmeng, Zhai Changhai and Xie Lili (2008), "An Improved Modal Pushover Analysis Procedure for Estimating Seismic Demands of Structures," *Journal of Earthquake Engineering and Engineering Vibration*, **7**(1): 25–31.

Marusic D and Fajfar P (2005), "On the Inelastic Seismic Response of Asymmetric Buildings under Bi-axial Excitation," *Earthquake Engineering and Structural Dynamics*, **34**: 943–963.

Moghadam AS and Tso WK (1998), "Pushover Analysis for Asymmetrical Multi-storey Buildings," *Proceedings of the 6th U.S. National Conference on Earthquake Engineering*, EERI, Oakland, CA.

Moghadam AS and Tso WK (2000), "Pushover Analysis for Asymmetric and Set-back Multi-storey Buildings," *Proceeding of the 12th World Conference on Earthquake Engineering*, Auckland, New Zealand, Paper No. 1093.

Moghadam AS (2002), "A Pushover Procedure for Tall Buildings," *Proceeding of 12th European Conference on Earthquake Engineering*, Paper 395, Elsevier Science Ltd., London, UK.

Mwafy AM and Elnashai AS (2001), "Static Pushover Versus Dynamic Analysis of R/C Buildings," *Engineering Structures*, **23**: 407–424.

Perus I and Fajfar P (2005), "On the Inelastic Torsional Response of Single-storey Structures under Bi-axial Excitation," *Earthquake Engineering and Structural Dynamic*, **34**(8): 931–941.

Poursha M, Khoshnoudian F and Moghadam AS (2009), "A Consecutive Modal Pushover Procedure for Estimating the Seismic Demands of Tall Buildings," *Engineering Structures*, **31**: 591–599.

Poursha M, Khoshnoudian F and Moghadam AS (2011), "Evaluation of Consecutive Modal Pushover Procedure for Nonlinear Static Analysis of One-way Asymmetric-Plan Tall Building Structures," *Engineering Structures*, **33**(9): 2417–2434.

Sasaki KK, Freeman SA and Paret TF (1998), "Multi-mode Pushover Procedure (MMP) – A Method to Identify the Effects of Higher Modes in a Pushover Analysis," *Proceeding of 6th U.S. National Conference on Earthquake Engineering*, Seattle, Washington.

Standard No. 2800-05 (2005), "Iranian Code of Practice for Seismic Resistant Design of Buildings," 3rd ed, Building and Housing Research Centre, Iran.

Tso WK and Moghadam AS (1998), "Pushover Procedure for Seismic Analysis of Buildings," *Progress in Structural Engineering and Materials*, **1**(3): 37–44.